Research Paper

A New Polymer–Lipid Hybrid Nanoparticle System Increases Cytotoxicity of Doxorubicin Against Multidrug-Resistant Human Breast Cancer Cells

Ho Lun Wong,[1] Andrew M. Rauth,[2] Reina Bendayan,[1] Janet L. Manias,[1] Manisha Ramaswamy,[1] Zengshe Liu,[3] Sevim Z. Erhan,[3] and Xiao Yu Wu[1,4]

Purpose. This work is intended to develop and evaluate a new polymer–lipid hybrid nanoparticle system that can efficiently load and release water-soluble anticancer drug doxorubicin hydrochloride (Dox) and enhance Dox toxicity against multidrug-resistant (MDR) cancer cells.

Methods. Cationic Dox was complexed with a new soybean-oil-based anionic polymer and dispersed together with a lipid in water to form Dox-loaded solid lipid nanoparticles (Dox–SLNs). Drug loading and release properties were measured spectrophotometrically. The *in vitro* cytotoxicity of Dox–SLN and the excipients in an MDR human breast cancer cell line (MDA435/LCC6/MDR1) and its wild-type line were evaluated by trypan blue exclusion and clonogenic assays. Cellular uptake and retention of Dox were determined with a microplate fluorometer.

Results. Dox–SLNs were prepared with a drug encapsulation efficiency of 60–80% and a particle size range of 80–350 nm. About 50% of the loaded drug was released in the first few hours and an additional 10–20% in 2 weeks. Treatment of the MDR cells with Dox–SLN resulted in over 8-fold increase in cell kill when compared to Dox solution treatment at equivalent doses. The blank SLN and the excipients exhibited little cytotoxicity. The biological activity of the released Dox remained unchanged from fresh, free Dox. Cellular Dox uptake and retention by the MDR cells were both significantly enhanced ($p <$ 0.05) when Dox was delivered in Dox–SLN form.

Conclusions. The new polymer–lipid hybrid nanoparticle system is effective for delivery of Dox and enhances its efficacy against MDR breast cancer cells.

KEY WORDS: breast cancer cells; doxorubicin delivery; *in vitro* cytotoxicity; multidrug resistance; polymer–lipid hybrid nanoparticles.

INTRODUCTION

Drug resistance is a common cause of treatment failure in the management of several cancer types including breast cancer (1,2). There are multiple mechanisms that underlie clinical drug resistance, including noncellular and cellular mechanisms. One of the most studied cellular mechanisms is the classical form of multidrug resistance (MDR), which is usually mediated by the overexpression of P-glycoprotein (P-gp) and other membrane transporters (3). P-gp is a membrane drug efflux transporter that reduces intracellular levels of a number of structurally unrelated compounds (4), including doxorubicin (Dox), a broad-spectrum cytotoxic anticancer drug commonly included in the regimens of breast cancer treatment (5). This transporter has been detected in

63% of patients with untreated breast cancer (4). An increase in P-gp expression in breast cancer after chemotherapy has also been correlated with lower clinical response rates (6).

To overcome drug resistance and to improve the effectiveness and safety of cancer chemotherapy, new drug delivery systems such as microspheres, nanoparticles, and liposomes have been studied (7–20). In comparison to the conventionally used drug solutions, these systems generally exhibit lower toxicity and thus allow higher doses of drugs to be safely administered. This is of clinical significance because many cytotoxic agents have low therapeutic indices.

Recently, encapsulated formulations of cytotoxic drugs and/or compounds with P-gp inhibitory activity have been studied for drug-resistant cancer treatment (7,15–20). Among these formulations, colloidal drug carriers have found particular use in reversing MDR phenotypes. Some of the colloidal drug carriers could be engineered to remain in the circulation for longer times or yield higher tumoral drug concentrations without significant toxicity and pharmacokinetic interactions compared to free drugs (13,18). Furthermore, studies performed on both noncancerous and cancerous tissues have demonstrated that some particulate formulations, even without loaded drug, possess "built-in" MDR reversal properties (21–31). In fact, it has long been recognized that

[1] Leslie Dan Faculty of Pharmacy, University of Toronto, 19 Russell Street, Toronto, Ontario, Canada M5S 2S2.
[2] Ontario Cancer Institute, 610 University Avenue, Toronto, Ontario, Canada M5G 2M9.
[3] Food and Industrial Oil Research, USDA/ARS/NCAUR, 1815 N. University Street, Peoria, Illinois 61604, USA.
[4] To whom correspondence should be addressed. (e-mail: xywu@phm.utoronto.ca)

nanoparticles are able to deliver drugs across the P-gp rich blood–brain barrier without damaging its structural integrity (21). There were also reports of enhanced cytotoxicity of anticancer drugs toward drug-resistant cancer cells when these drugs were loaded into polymeric systems (22,23) or some forms of liposomes (24–26). In these studies, inhibition of P-gp by lipids or nonionic surfactants used in the formulations were identified or suggested as a possible mechanism for the enhanced toxicity in cancer cells.

Solid lipid nanoparticles (SLNs) are colloidal drug carriers with great potential to improve chemotherapy of MDR cancer, yet this area remains largely unexplored. SLNs have good handling properties, very low intrinsic toxicity toward noncancerous tissues, potential to be surface-engineered, and manageable burst effect issues that are commonly associated with many colloidal formulations (27,28). The drug-loading mechanisms of SLN are relatively nonspecific, allowing them to deliver structurally diverse lipophilic, water-insoluble compounds. Recently SLNs have been studied for the delivery of a water-insoluble cytotoxic agent, paclitaxel, to brain tumors (29). However, for loading highly water soluble, ionic drugs such as Dox hydrochloride, SLN formulations face challenges owing to low drug partitioning in the lipid phase. A previous study has attempted the use of organic anions to form ion pairs with Dox for the improvement of drug lipophilicity and drug loading (30). This SLN formulation was shown to exhibit higher toxicity against colorectal cancer and breast cancer cell lines than the conventional Dox solution as determined by the trypan blue assay (31,32). Despite these encouraging results, some issues remain to be addressed. It seems that the reported SLN formulation provided a very low release rate of Dox with only 0.1% of Dox being released after 2 h, perhaps due to the high lipophilicity of the Dox–ester ion pairs as the authors suggested, and no release profile for longer times was studied (30). Although slow drug release may lead to lower systemic toxicity, continuous exposure to low levels of cytotoxic agents may induce P-gp overexpression (33), which may render the cancer cells more drug resistant. Moreover, higher drug doses are required to kill MDR cells than nonresistant cells because of the elevated efflux. To this end, an SLN formulation with higher drug release rates may be desirable.

In our previous research, we have developed a new polymer–lipid hybrid formulation of SLNs consisting of dextran sulfate, an anionic polymer that can form complexes with a range of cationic drugs (34). Increased drug loading has been obtained for cationic drugs including Dox. Up to 90% of the loaded Dox was released in 18 h by using a combination of ion-exchange and diffusion-controlled mechanisms. The results lead to a speculation that this polymer–lipid nanoparticle system may suit the purpose of MDR cancer treatment.

In this work, we further improved the formulation of the SLN-containing Dox (Dox–SLN) by using a new anionic polymer to achieve better particle morphology and drug-loading capacity. Furthermore, we investigated for the first time the effect of the polymer–lipid hybrid SLN system on the cytotoxicity of Dox against human MDR breast cancer cells (MDA435/LCC6/MDR1). This cell line was chosen because it highly expresses a classical membrane transporter, P-gp–MDR1 by transduction of MDA435/LCC6 cell line

with a retroviral vector directing the constitutive expression of the MDR1 cDNA (35). Besides, its wild-type parent cell line is available for comparative studies. Clonogenic assay was employed in this work in addition to trypan blue exclusion assay to evaluate the cytotoxicity of the SLN system. Although trypan blue exclusion assay is adequate for testing the acute effects of the formulations on cell membrane integrity and was solely used for the evaluation of cytotoxicity in the previous studies of Dox-encapsulated SLNs (30–32), clonogenic assay is traditionally the gold standard for the evaluation of longer-term effects on cancer cell proliferation (36). The combination of the two assays may provide a more complete picture of the anticancer activities of the new SLN formulation.

MATERIALS AND METHODS

Materials

Epoxidized soybean oil (ESO) used for polymer synthesis was obtained from Elf Atochem Inc. (Philadelphia, PA, USA) and used as received. Boron trifluoride diethyl etherate $(C_2H_5)_2OBF_3$, purified and redistilled, was provided by Aldrich Chemical Co. Inc. (Milwaukee, WI, USA). Methylene chloride was purchased from Fisher Scientific (Fair Lawn, NJ, USA).

The Pluronic F68 was a gift from BASF Corp. (Florham Park, NJ, USA). Doxorubicin HCl, rhodamine-B, stearic acid, and other chemicals used, unless otherwise specified, were all purchased from Sigma-Aldrich Ltd. (Oakville, ON, Canada). Distilled and deionized (DDI) water was prepared with a Millipore water-purification system (Etobicoke, ON, Canada).

Tumor Cell Lines and Culture

A human breast carcinoma cell line that expresses high level of P-gp (MDA435/LCC6/MDR1) and its parent line (MDA435/LCC6/WT) were kindly provided by Dr. R. Clarke (Georgetown University, Washington, DC, USA). All cell lines were grown as monolayers in 75-cm^2 polystyrene tissue culture flasks in a mixture of 5% CO_2 and 95% humidified air at 37°C, in α-minimal essential medium (α-MEM, Ontario Cancer Institute Media Lab, Toronto, ON, Canada), pH 7.2, supplemented with 10% fetal bovine serum (Cansera Inc., Etobicoke, ON, Canada) and 0.5% penicillin/streptomycin suspension (growth medium). Confluent cultures were trypsinized with 0.05% trypsin–EDTA (Invitrogen Inc., Burlington, ON, Canada), diluted (1/10) in fresh growth medium, and subcultured on a weekly basis. All experiments were conducted on confluent, cell monolayers from passages 5 to 30 after receipt of cells. The presence of high levels of P-gp in the MDA435/LCC6/MDR1 cell line was confirmed with the use of Western blot analysis (results not shown).

Synthesis of Hydrolyzed, Polymerized Epoxidized Soybean Oil Polymer

Hydrolyzed polymer of epoxidized soybean oil (HPESO) was synthesized by using a method described in detail

elsewhere (37). Briefly, (C$_2$H$_5$)$_2$OBF$_3$ was added dropwise to a 10% ESO solution in methylene chloride at 0°C to initiate ring-opening polymerization. After 3 h of reaction, the solvent was evaporated under vacuum at 70°C. The resultant polymer was hydrolyzed by refluxing with 0.4 N sodium hydroxide for 24 h. The hydrolyzed product was precipitated with 1 N hydrochloride acid and washed with copious amounts of water several times and then with 10% v/v acetic acid to remove the residual hydroxide. The polymer with a structure shown in Fig. 1 was then dried under vacuum for storage. The number and weight average molecular weights of the polymer were determined by gel permeation chromatography and found to be M_n = 3160 and M_w = 4866. Aqueous HPESO solutions were prepared by dissolving the polymer in DDI water and filtering with 0.22-μm filter for sterilization and removal of particulate matter prior to the preparation of nanoparticles and the toxicity evaluation.

Partition of Dox in Lipid–Polymer–Water System

A drug partition study was conducted to evaluate whether the lipid–polymer combination of choice has the potential to efficiently incorporate Dox. Stearic acid was heated with an aqueous solution of HPESO polymer to 75°C under constant stirring. Dox solution was added dropwise (Dox-to-polymer w/w ratio = 2:1) to the lipid–polymer mixture. Distilled water preheated to the same temperature was added to adjust the lipid-to-water w/w ratio in the system to 1 to 9. After lipid–water phase separation, samples of the aqueous phase were drawn and the amount of Dox was measured by UV–Vis spectrophotometry (Agilent 8453 UV–visible spectrophotometer, Walbronn, Germany) at 498 nm. The percentage of Dox partitioned in the lipid phase was determined using the equation: (total amount of Dox − amount of Dox in aqueous phase) × 100%/total amount of Dox.

Preparation of SLNs and Drug–Polymer Aggregates Containing Dox

Dox–SLNs were prepared similarly to a previous study (34), with the addition of an ultrasonication step for improved lipid dispersion (38). Briefly, a mixture of 50 mg stearic acid and 0.45 mL of aqueous solution containing 0.5 to 5 mg Dox and Pluronic F68 (2.5% w/v) was warmed to 72–75°C in a water bath. HPESO polymer solution preheated to 75°C was added to the mixture (Dox/polymer w/w ratio = 2:1). The final mixture formed was stirred for 10 min and then ultrasonicated for 3 min to form submicrometer-sized lipid emulsion. Dox–SLNs were formed by dispersing 1 volume of the emulsion in 4 to 9 volumes of water at 4°C. Blank SLNs were prepared in the same manner except Dox was omitted.

Dox–HPESO aggregates were prepared by magnetically stirring the mixture of aqueous solutions of Dox and HPESO in 2:1 w/w (Dox/polymer) ratio in the dark until a suspension of fine aggregates was formed. The suspension was centrifuged at 1.000 × g for 2 min. The supernatant containing the uncomplexed drugs were drawn out and the pellet was washed with ice-cold distilled water. The washout liquid was pooled with the supernatant and the amount of uncomplexed Dox was measured by spectrophotometry from which the complexed drug was calculated. It was estimated that 67% of Dox was complexed with the polymer (data not shown). Dox–HPESO pellets were resuspended in 2.5% Pluronic F68 and diluted to the desired concentrations for the cytotoxicity tests.

Measurement of Size, Morphology, and Surface Charge of Nanoparticles

The particle size distribution and zeta potential were measured by photon correlation spectroscopy (PCS) with a zeta potential analyzer add-on unit (Nicomp Zetasizer 380ZLS, Urbana, IL, USA). Samples of SLN were diluted to the desired concentration with water prior to the measurements and two 5-min cycles were run for each sample. Intensity-weighted size distributions are reported. For zeta potential measurements, three 30-s cycles were run for each sample. The morphology of SLN was examined by transmission electron microscopy (TEM) (Hitachi 7000H, Tokyo, Japan) following negative staining with phosphotungstic acid.

Measurement of Drug-Loading and Drug-Release Kinetics of Dox–SLN

A filtration method, as described in a previous study (34), was used to determine the drug loading of Dox–SLN. Typically, freshly prepared samples of Dox–SLN suspension were filtered with 0.1-μm filter units. Dox concentration in the filtrate was measured by UV–Vis spectrophotometry at 498 nm. The measurements were compared to the calibration curves prepared using standard Dox solutions that were filtered in the same manner to correct for Dox adsorption onto the filters. The amount of loaded Dox was calculated using the equation: (total weight of drug added − calibrated drug concentration in filtrate × total volume of SLN suspension). The percent drug loading (% DL) and drug encapsulation efficiency (EE) was calculated by using the following equations, respectively:

$$\%DL = (W_{DL} \times 100\%)/W_{SLN}$$

$$EE = (W_{DL} \times 100\%)/W_D$$

where W_{DL} = weight of drug loaded in SLN, W_{SLN} = weight of SLN, and W_D = weight of drug added to the preparation.

To establish the drug release kinetics, 5 mL of freshly prepared suspension containing 100 mg Dox–SLN (or 5 mL of Dox–HPESO containing 3.5 mg Dox) was added to 95 mL of phosphate-buffered saline (PBS, pH 7.4, μ = 0.15 M) preheated to 37°C to initiate the drug release. The resulting suspension was magnetically stirred in darkness. Aliquots of suspension were sampled at specified time points and the Dox concentrations present in the release medium (C_t) were determined by the filtration method described above (32). In addition, to correct for the concentration of the unloaded, free drug (C_u) that was initially present, 0.5 mL freshly prepared SLN suspension was added to 9.5 mL distilled water at 4°C, the mixture formed was immediately filtered, and the unloaded Dox concentration in the filtrate was determined. The amount of the released drug at
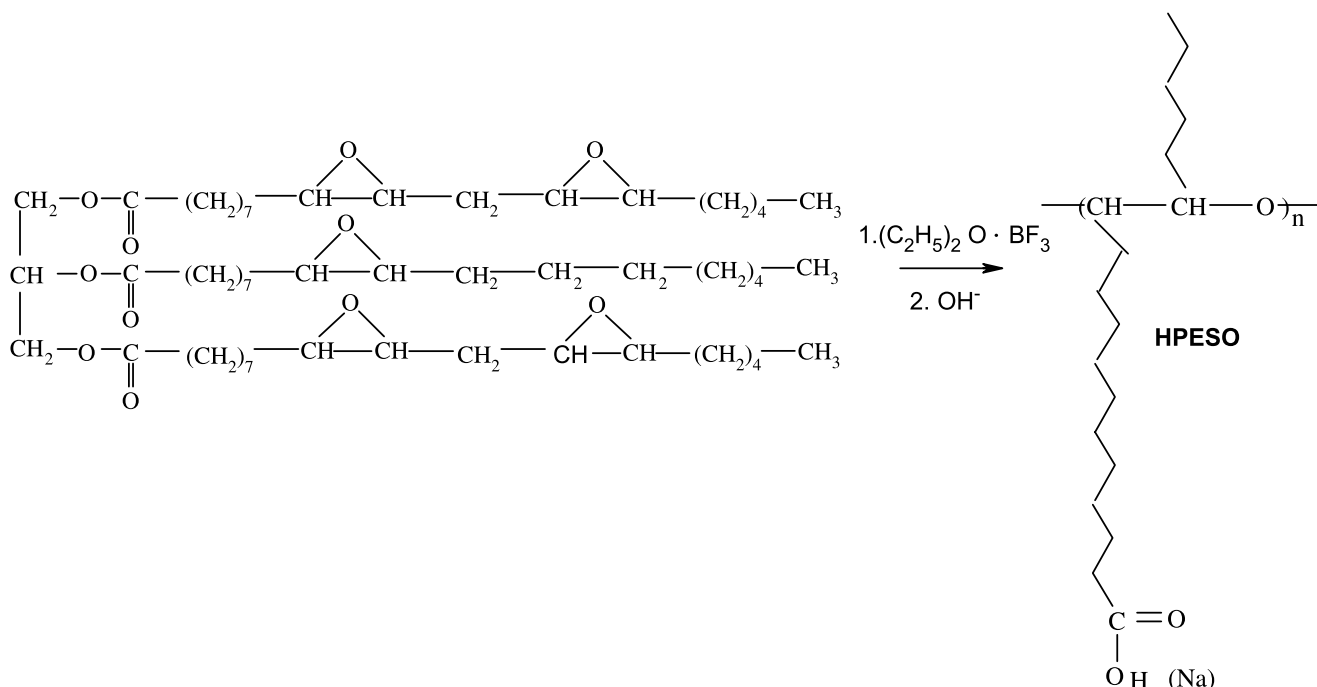
Fig. 1. Synthesis of HPESO polymer. Epoxidized soybean oil was polymerized by boric trifluoride diethyl etherate, and then hydrolyzed with sodium hydroxide to form HPESO.

each time point was then calculated as $(C_t - C_u) \times$ total volume of diluted suspension and plotted as the drug release profile.

Trypan Blue Exclusion Assays

Trypan blue exclusion assays were carried out as previously described (7) to evaluate the acute cellular toxicity of SLNs and other tested agents. Confluent cells were trypsinized, adjusted to the desired cell concentration with growth medium, and treated with blank SLN, Dox–SLN, HPESO polymer, Dox–HPESO aggregates, or Pluronic F68 in PBS. Aliquots of the treated cells (2 mL cell suspension containing 2×10^6 cells) were transferred to sterile polypropylene tubes and incubated at cell culture conditions ($37°C$, 5% CO_2) under constant mechanical shaking. Samples of cell suspension were collected after 1, 4, 8, and 24 h of incubation and treated with 0.4% trypan blue in 0.9% saline for 5 min. Stained, nonviable cells, and unstained, viable cells, were counted in a hemocytometer. Membrane integrity of the tested cells was calculated using the equation: membrane integrity = (number of viable treated cells)/(total number of cells). The results were normalized against that of the control (untreated cells).

Clonogenic Assays

Clonogenic assays were performed to evaluate the effectiveness of the tested treatments on cancer cell proliferation (36). Approximately 5×10^5 human breast cancer cells trypsinized at confluence were seeded into 10-cm plastic Petri dishes. Cultures were initiated 24 h before the experiments. Aliquots of agents to be tested were introduced to the dishes and cells were incubated for 1 or 4 h. Treatments included 1) Dox solution, 2) Dox released from SLN, 3) Dox–HPESO

aggregates, 4) Dox–SLN, and 5) blank SLN. Dox released from SLN was obtained by incubating Dox–SLN in PBS at $37°C$ for 24 h and removing the particulate matter by centrifugation at $120,000 \times$ g for 30 min. The supernatants containing the released Dox were adjusted to the desired drug concentrations based on their light absorbance at 498 nm. Dox–SLN, blank SLN, and Dox–HPESO were prepared as previously described. The doses of Dox in Dox–SLN suspension were calculated using the payload plus unbound drug previously determined. In all cases, treatments were terminated by washing the cells with cold PBS three times. Treated cells were trypsinized, plated on 6-cm Petri dishes (100, 1,000, or 10,000 cells per dish in duplicate), and
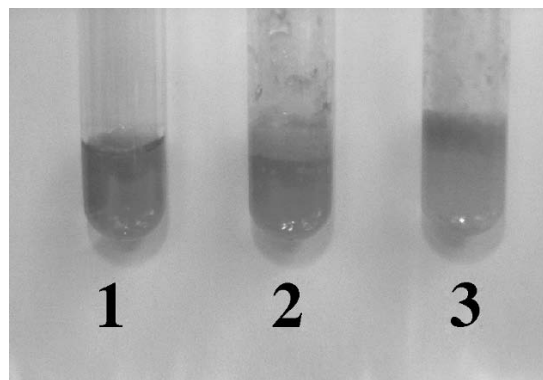

Fig. 2. Distribution of Dox in lipid–water system, with or without adding HPESO. (1) Dox solution only; (2) Dox solution (0.9 mL) + stearic acid (0.1 g); (3) Dox solution (0.9 mL) + stearic acid (0.1 g) + HPESO polymer (0.45 mg). In all samples, Dox concentration was 1 mg/mL. The mixture was warmed with stirring to $75°C$ for 15 min and then allowed to achieve phase separation.
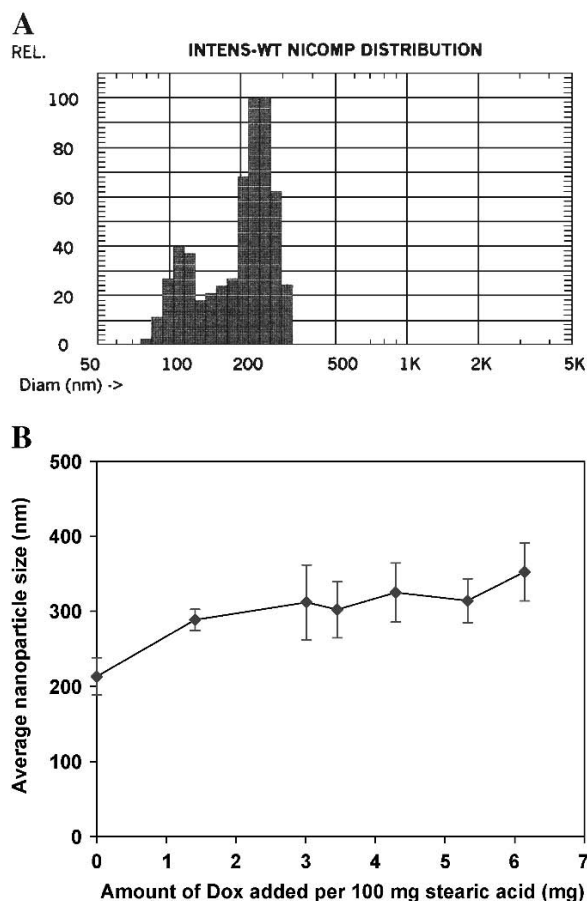
A

REL.

INTENS-WT NICOMP DISTRIBUTION

Diam (nm) ->

B

Fig. 3. (A) A representative size distribution of Dox–SLN measured by photon correlation spectroscopy (Note the *x* axis is a log scale). The Dox–SLN sample contains 3.5% w/w Dox; (B) Average size of nanoparticles at increasing percent w/w Dox loading per particle as measured by photon correlation spectroscopy. Each value is expressed as mean ± SD, $n = 3$ ($n = 5$ for blank particles).

incubated in growth medium under cell culture conditions. After 10 to 14 days the macroscopic colonies formed from viable cells were fixed and stained with 0.5% solution of methylene blue in ethanol and their numbers were counted. Plating efficiency (PE) of each treatment was calculated as (number of colonies formed × 100%)/(number of cells plated). The results were reported as normalized PE, which were determined by dividing the PE of the treated cells by the PE of the control (untreated cells). The PE of the untreated MDA435/LCC6/WT and MDA435/LCC6/MDR1 cells were found to be 29.2 ± 7.9 and 34.1 ± 6.8% (mean ± SD), respectively. For every concentration point of each treatment, six samples were prepared. The experiments were repeated at least three times with cells from different passages.

Cellular Uptake and Retention of Doxorubicin

To evaluate cellular Dox uptake, MDA435/LCC6/WT and MDA435/LCC6/MDR1 cells were plated onto 48-well plates at densities of approximately 40,000 to 100,000 cells/ well at 37°C. When cells reached confluence, they were incubated with Dox solution only, Dox solution combined

with blank SLN, or Dox–SLN suspension at cell culture conditions. Treatments were all diluted to 10 µg/mL Dox concentration using Earle's balanced salt solution (EBSS). Blank EBSS was used as the negative control. After 4 h treatment, cells were rinsed with ice-cold PBS (pH 7.6) three times and lysed with PBS containing 1% Triton-X. SpectraMax Gemini XS microplate fluorometer (Molecular Devices, Sunnyvale, CA, USA) at an excitation wavelength $\lambda_{ex} = 478$ nm and an emission wavelength $\lambda_{em} = 594$ nm to measure the Dox concentrations in the cell lysates. Results are expressed as nanomoles per milligram of protein. Protein concentrations of the cell lysates were determined by Bradford colorimetric assay using reagents from BioRad (Melville, NY, USA) and bovine serum albumin (Sigma-Aldrich Inc., Mississauga, ON, Canada) as the standard.

To evaluate the quantities of Dox retained by cancer cells after a drug efflux period, procedures similar to the drug uptake assay were employed, except after 2 h of treatment with Dox solution or Dox–SLN (adjusted to 10 µg/mL Dox), cells were rinsed with PBS three times and reincubated with fresh, drug-free EBSS for another 2 h to allow drug efflux from the cells. At the end of drug efflux, the EBSS containing the effluxed drugs was washed away, cells were lysed, and the amount of cellular Dox was measured by a microplate reader as previously described. Cellular Dox amounts prior to the drug efflux were also measured. Results are expressed as percent Dox retained by cells after drug efflux, whereby each measurement was normalized against the measurement of the corresponding cell line/treatment prior to the 2 h drug efflux period.

Data Analysis

Analysis of the clonogenic assay results for various treatment groups compared with the free Dox group was carried out using two-way ANOVA with independent samples. Student's *t* test was performed to compare the particle size of nanoparticle formulations to the control
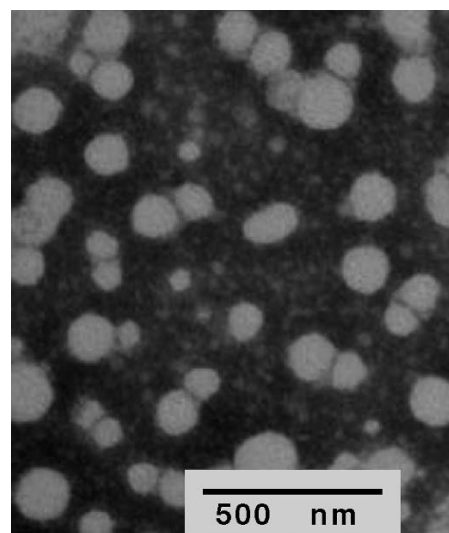

Fig. 4. Transmission electron microscopy (TEM) image of Dox–SLN (40,000× magnification). The particles were negatively stained with aqueous solution of phosphotungstic acid (PTA) 5 min prior to imaging. The sample used was loaded with 3.8% w/w Dox.
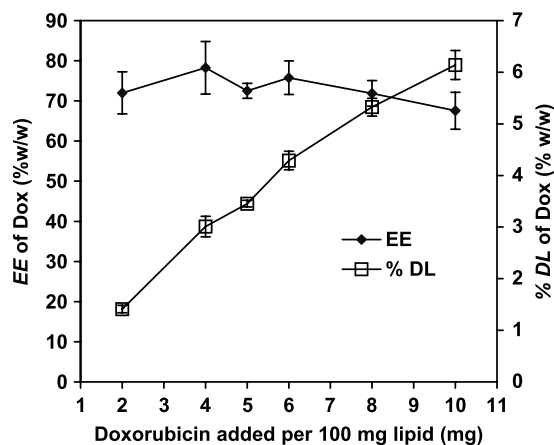
Fig. 5. Effect of the amount of drug fed in Dox–SLN preparation on drug encapsulation efficiency (*EE*) and percent of drug loading (% *DL*). Results were expressed in terms of Dox loaded per weight of nanoparticles in Dox–SLN as a function of amount of Dox in the feed per 100 mg of lipid. Each value represents mean ± SD ($n \geq 3$).

(blank nanoparticles). In all analyses, $p < 0.05$ was considered significant unless otherwise specified.

RESULTS

Partition of Dox in Lipid–Polymer–Water System

Figure 2 presents the visual change in Dox distribution from a pure water system (system 1) to two different lipid–water systems: stearic acid–water (system 2) and stearic acid, HPESO–water (system 3). When compared to the system without HPESO polymer (system 2), the addition of HPESO (system 3) visibly enhances the Dox partitioning in the lipid (the upper phase). The spectrophotometry data showed that with the addition of HPESO, the percentage of Dox partitioned in the lipid phase increased from 23.1 ± 0.9 to 71.9 ± 3.6% ($p < 0.001$) and from 18.1 ± 1.6 to 67.1 ± 3.9% ($p < 0.001$) for 1 and 5 mg of Dox in 100 mg of stearic acid, respectively.

Size, Morphology, and Surface Charge of Nanoparticles

Figure 3A shows a typical particle size distribution of a Dox–SLN sample with 3.5% Dox loading (w/w) measured by PCS. The mean particle size ($n = 5$ for blank SLN, $n = 3$ for other samples) is about 200 to 350 nm, which slightly increases with increasing drug loading (Fig. 3B), and the range of the particle size in the sample is about 80 to 350 nm. The TEM image of a Dox–SLN sample (Fig. 4) illustrates that the particles are generally spherical in shape and the majority of the particles are in the range 50 to 200 nm in diameter, which are smaller than those determined by PCS. This discrepancy is probably due to the difference in the measurement conditions. For PCS measurement, particles are dispersed in water. They may absorb water, swell, and become larger due to the presence of the polymer (33). In addition, PCS measures hydrodynamic sizes of particles, which include both the solid particles and the hydration surface layer. In contrast, during TEM measurement, the

particles are exposed to high vacuum and dehydrated and are therefore smaller (39).

The average values of zeta potential of blank SLN and Dox–SLN with 4% drug loading in water were −23.1 ± 0.28 mV ($n = 6$) and −19.7 ± 0.65 mV ($n = 6$), respectively. The negative surface charge is indicative of the exposure of the anionic HPESO chains on the surface. In the presence of Dox, some of the negative charges are neutralized by the complex formation, leading to less negative zeta potential.

Drug Loading and Encapsulation Efficiency

Figure 5 presents the percent drug loaded per weight of nanoparticle (% DL) and encapsulation efficiency of Dox (EE) in Dox–SLN as a function of Dox added per 100 mg of the lipid. As the amount of Dox is increased from 2 to 10 mg, % DL progressively increases from less than 2 to above 6% w/w. EE remains between 70 to 80% up to 6 mg of Dox added and only declines slightly to about 65% up to 10 mg of Dox added. In the absence of the anionic polymer, the EE values were 38 and 28%, respectively ($n = 2$ in each case, data not shown), for SLNs prepared with 2 and 5 mg of Dox per 100 mg of lipid.

Drug Release Kinetics of Dox–SLN and Dox–HPESO

A typical drug release profile of Dox–SLN with 3.5% drug loading is shown in Fig. 6. Half of the drug loaded in the nanoparticles is released in about 2 to 4 h, and an additional 10% of the loaded drug is gradually released in another 12 h. The total amounts of drug released from the nanoparticles after 72 h and 2 weeks (not shown in the graph) were 66.2 ± 4.1 and 70.6 ± 4.5% ($n = 3$, mean ± SD), respectively. For comparison, the drug release profile from Dox–HPESO was also obtained. A quick release was observed with approximate 35% of Dox being released in 15 min and a plateau at about 40% reached after 1 h.
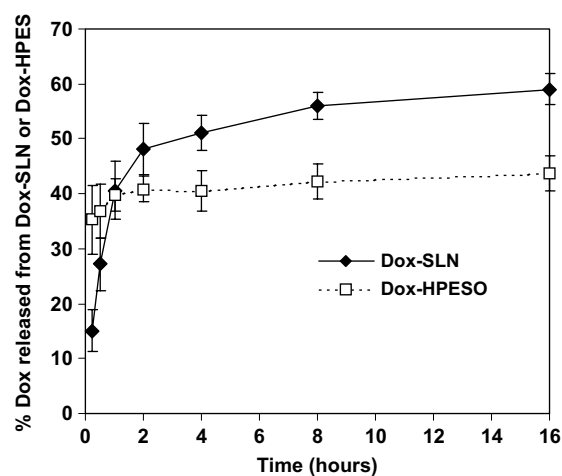

Fig. 6. Drug release profiles of Dox from Dox–SLN (average drug loading of three different batches = 3.5% w/w) or Dox–HPESO (containing 3.5 mg Dox in 5 mL) in PBS (pH 7.4, μ = 0.15 M) at 37°C. Not shown in the Dox–SLN profile are the values of percent Dox released after 72 h and 2 weeks, which were measured as 66.2 ± 4.1 and 70.6 ± 4.5%, respectively. Each value represents mean ± SD of the measurements obtained in three separate experiments.
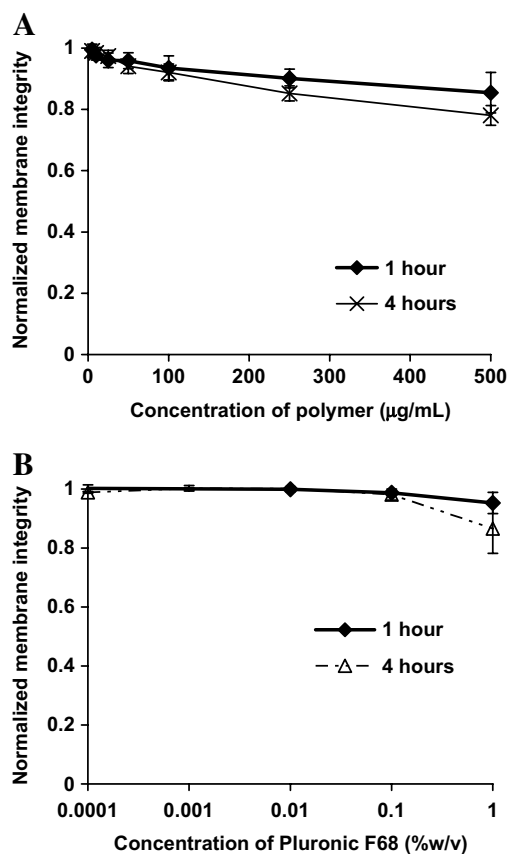
Fig. 7. Results of trypan blue exclusion assay experiments showing the effects of free HPESO polymer and Pluronic surfactant used in Dox–SLN preparation on cancer cell membrane integrity. MDA435/LCC6/WT cells were exposed to (A) HPESO, and (B) Pluronic F68 solution at various concentrations in PBS for 1 or 4 h. Results were normalized against the control (PBS without polymer and surfactant). Each value represents mean ± SD of measurements obtained in three separate experiments ($n = 2$ in each experiment).

Influence of Dox–SLNs and Various Treatments on Cell Membrane Integrity

Figures 7A, B and 8A, B present results for cell membrane integrity after various treatments with Dox–SLN and its components including HPESO and Pluronic F68 determined by trypan blue exclusion assays. As illustrated in Fig. 7A, the normalized membrane integrity of MDA435/LCC6/WT cells treated with HPESO polymer for 1 or 4 h are close to 100% when the concentration is 10 μg/mL or less, which are the typical polymer concentrations present in the SLN treatments. Cell membrane integrity remains over 80% even at polymer concentrations up to 500 μg/mL. Figure 7B shows that when 0.1% w/v or less Pluronic F68 is used in the SLN preparation, the cell membrane integrity is nearly the same as that of the control even after 4 h of exposure. As the concentration of the surfactant is increased to 1% w/v for 4 h, approximately 90% of the cells still remain intact. Note that the concentrations used in Fig. 7B are much higher than the highest concentration of Pluronic F68 used in the clonogenic assays, i.e., 0.005% w/v.

As shown in Fig. 8A and B, Dox–SLN and the components of the formulation (HPESO polymer, Dox,

Dox–HPESO, blank SLN) do not significantly reduce the normalized membrane integrity of either wild-type (Fig. 8A) or drug-resistant (Fig. 8B) cancer cells for exposures of 4 h or less to below 1 ($p > 0.05$). Decreases in normalized membrane integrity ($p < 0.05$) are seen only in the treatments that contain Dox (Dox, Dox–HPESO, and Dox–SLN) for longer periods of time (8 and 24 h). These decreases are larger in the wild-type cells (Fig. 8A) than in the MDR cells (Fig. 8B).

Effects of Dox–SLN and Other Treatments on Cell Survival

The effects of the exposure to Dox or other treatments on cell survival measured by a clonogenic assay are shown in Figs. 9 and 10A and B. Figure 9 compares the normalized PE of wild-type cells treated with Dox released from Dox–SLN and fresh Dox solution of various concentrations. The released Dox exhibits the same cytotoxicity as
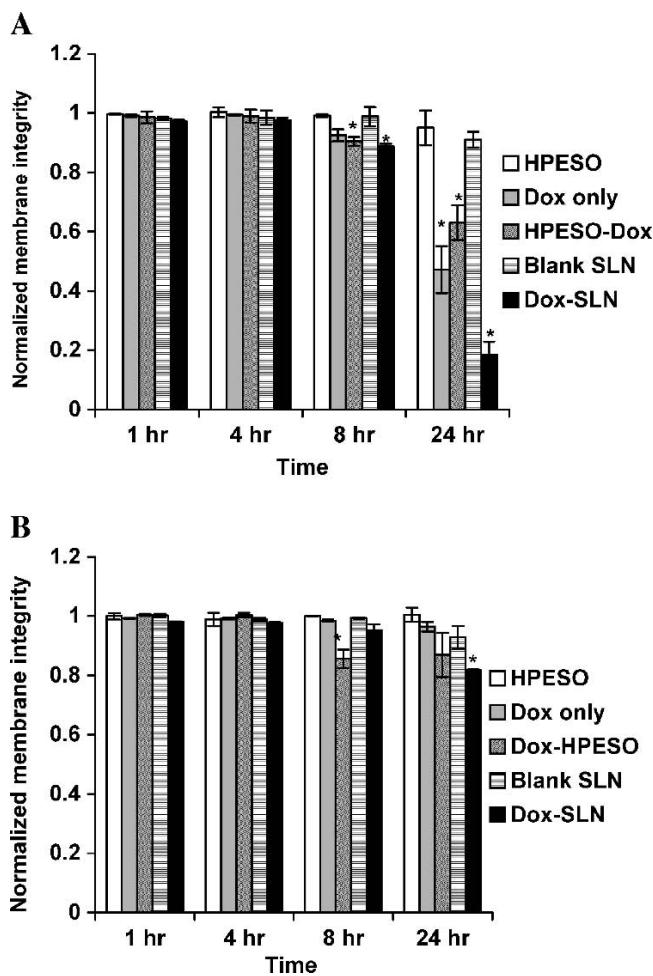

Fig. 8. Results of trypan blue exclusion assay experiments showing the effects of HPESO solution, Dox–HPESO aggregates, blank SLN, and Dox–SLN on cell membrane integrity of (A) MDA435/LCC6/WT cells and (B) MDA435/LCC6/MDR1 cells. Cells were treated for 1, 4, 8, and 24 h. The total concentrations of Dox, HPESO polymer, and stearic acid used were 10, 5, and 200 μg/mL, respectively. Results were normalized against the control (drug-free PBS). Each value represents mean ± SD of the measurements obtained in three separate experiments ($n = 2$ in each experiment). *$p < 0.05$, normalized membrane integrity significantly lower than 1.
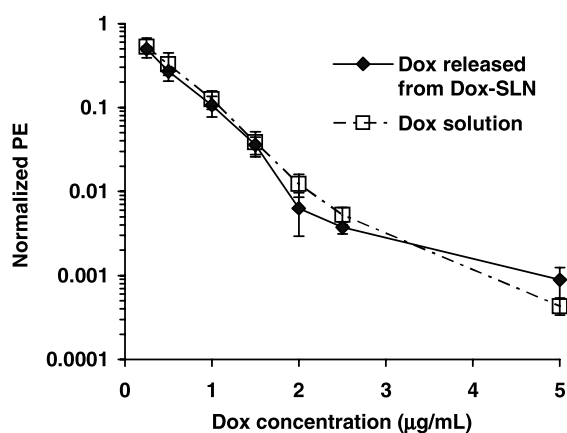
Fig. 9. Comparison of the biological activities of Dox released from Dox–SLN to fresh standard Dox solution. Activity was determined by measuring the cell plating efficiency of MDA435/LCC6/WT cells using a clonogenic assay. Results were normalized against the control (cells treated with PBS in α-MEM) and expressed in terms of normalized plating efficiency (normalized PE). Drug exposure time = 1 h. Each value represents mean ± SD of the measurements obtained in three separate experiments ($n = 6$ in each experiment).

the fresh Dox solution in the studied concentration range after 1 h exposure ($p > 0.05$).

Figure 10A and B compares the tumour cell toxicity of 4 h exposures to free DOX solution, Dox–HPESO polymer aggregates (Dox–polymer aggregates), Dox–SLN, and Dox plus blank SLN (blank SLN added separately to free Dox solution) on wild-type and MDR breast cancer cell lines, respectively. As expected, all four types of Dox-containing treatments are more cytotoxic to wild-type cells than to MDR cells; the normalized PE of MDR cells is at least one log scale higher than the wild-type cells receiving the same treatment type. Note that the range of Dox concentrations in Fig. 10A (0.5–5 μg/mL) is lower than those in Fig. 10B (1–10 μg/mL). As demonstrated in Fig. 10A, Dox–polymer aggregates were more cytotoxic than Dox solution ($p < 0.05$), whereas the cytotoxicity of Dox–SLN was similar to that of Dox solution. A different pattern is observed in the experiments with MDR cells (Fig. 10B). Dox–SLN treatment is significantly more toxic toward MDR cells than other treatments with over 8-fold cell kill being achieved in the higher concentration range. On the other hand, Dox–polymer aggregates exhibit no difference in cytotoxicity against MDR cells as compared to Dox solution. As seen in Fig. 10A and B, the addition of blank SLN to fresh Dox solution does not increase the cytotoxicity toward either cell type.

Effect of Dox–SLN on Cellular Drug Uptake and Drug Retention

Table I summarizes the results of cellular Dox uptake study. After 4 h of treatment, Dox–SLN led to moderately but significantly higher drug uptake ($p < 0.05$) by P-gp-overexpressing cells than Dox solution at the same drug concentration. The difference in Dox uptake between solution and SLN formulations is insignificant in wild-type cells. To determine if the particles themselves and the surfactants also played a role, Dox solution/blank SLN

combination was tested. No significant increase in Dox uptake was contributed by the blank SLN when compared to Dox only.

Figure 11 presents the results of cellular Dox retention study. Nearly 2-fold of Dox delivered by Dox–SLN was retained by P-gp-overexpressing cells after the 2-h drug efflux experiment when compared to cells treated with Dox solution. Again, no such improvement was observed in wild-type cells.

DISCUSSION

Efficient loading of water-soluble, ionic drugs using SLN has always been a tricky issue to solve. In this study, the
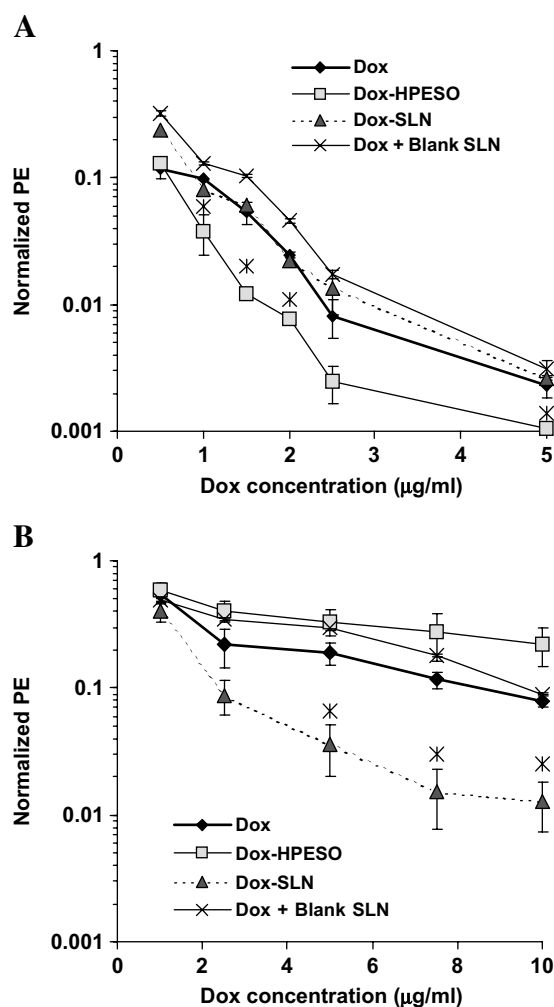

Fig. 10. Clonogenic assay experiments for the toxicity of Dox in (A) MDA435/LCC6/WT and (B) MDA435/LCC6/MDR1 cell lines. The normalized plating efficiencies (normalized *PE*) after 4 h exposure to Dox solution, Dox–HPESO aggregates, Dox–SLN, or Dox solution + blank SLN are shown. In treatments that included HPESO polymer (Dox–polymer aggregates and Dox–SLN) or lipid (Dox–SLN and Dox + blank SLN), the w/w ratios of polymer to Dox and lipid to Dox were equally set at 1:0.48 and 1:20, respectively, at all Dox concentrations. Results are expressed as mean ± SD of the measurements obtained in three separate experiments ($n = 6$ in each experiment). *$p < 0.05$, significantly different from Dox solution group.

Table I. Cellular Uptake of Doxorubicin by Wild-Type MDA435/LCC6/WT (WT) and P-gp-Overexpressing MDA435/LCC6/MDR1 (MDR) Breast Cancer Cell Lines Treated with Doxorubicin Solution Only (Dox), Dox + Blank SLN Combination, and Dox–SLN for 4 h

	Cellular Dox uptake (nmol drug/mg cellular protein)		
Cell line	Dox only	Dox + blank SLN	Dox–SLN
WT	924.4 ± 48.5	839.8 ± 81.2	985.0 ± 111.0
MDR	665.9 ± 50.9	581.3 ± 67.4	829.2 ± 42.7*

*$p < 0.05$, indicating statistically significant enhancement of Dox uptake in the MDR cells by the Dox–SLN formulation.

results demonstrate that the new, anionic polymer is able to enhance the partition and thereby the loading of Dox in the lipid nanoparticles. The use of HPESO that contains carboxylic groups has improved the quality of the SLN. As compared to the previous formulation consisting of a more hydrophilic polymer, dextran sulfate (DS) (34), the HPESO-containing SLNs were more uniform and more spherical. Unlike the SLNs made from DS which formed large agglomerates when the dug loading was over 4%, HPESO-containing SLN showed much less aggregation at Dox loading up to 6%. Only some slight increase in the particle size was observed at higher levels of drug loading (Fig. 3B). This property enables the preparation of Dox–SLN with higher drug loading than the DS-based system.

A significant amount of Dox, e.g., up to 60% in 16 h, was released from the present SLN system in the presence of counterions (Fig. 6). This release rate is lower than that of the previous DS-based system that delivered over 80% of Dox in 16 h (34), suggesting that HPESO and DS may be used alone or in combination to tailored drug release rate of a polymer–lipid hybrid nanoparticle system. Both the HPESO and DS-based SLN systems offer much higher release rates than the Dox–ester system (30) probably due to a major difference in the hydrophilicity between the counterions used in the SLN formulations. The role of the hydrophilic polymers in the release rate and release mechanisms of the hybrid SLN systems is being studied in our laboratory and will be reported in another paper.

In comparison to Dox–SLN, Dox–HPESO aggregates released a more substantial burst of drug at the beginning (Fig. 6), and did not release as much drug later on. Without a lipid barrier, the drug molecules that are bound to the surface of the polymer aggregates by ionic complexation can be rapidly released in the presence of counterions in the buffer. Because the aggregates are large (several micrometers to millimeters) and the polymers are densely packed, it is likely that a considerable portion of drug locked up in the inner cores of these aggregates is hardly available for release and contributes to the later slow-release phase. The finding again confirms the importance of lipids in the formulation.

Although trypan blue exclusion assay and clonogenic assay are sometimes considered as cytotoxicity assays, they serve different purposes in the present study. Trypan blue exclusion assay determines the short-term, nonspecific toxicity of the tested agent that causes loss of cell viability and subsequent alterations in the cell membrane properties. This method used alone, however, is relatively insensitive to cell injuries and may not indicate the long-term consequence of the treatment (40). Injured cells that have lost the reproductive potential, which is usually the major concern in cancer

chemotherapy, may still be able to exclude the dye. In this study, long-term cancer cell proliferation was measured using clonogenic assays. The difference between these two assay methods is evident when their results are compared (Figs. 8 and 10). In general, higher cytotoxicities were demonstrated using clonogenic assays, indicating that many cells that remained apparently viable in short term have suffered sufficient cell damage caused by the treatments leading to suppressed growth and proliferation.

Figure 8A and B shows significant decrease in membrane integrity only after 24 h of Dox-containing treatment (Dox solution, Dox–SLN, Dox–HPESO). Because both blank SLN and HPESO are nontoxic to the cells (Figs. 6 and 7), this toxicity was likely contributed by Dox in these formulations. Among the three Dox-containing formulations, Dox–SLNs are comparatively most toxic, even more toxic than Dox in wild-type cells. In addition to more Dox release from the nanoparticles, the extended duration of treatment (24 h instead of 4 h used in clonogenic assay) could possibly allow more cell–particle interactions. In fact, a mechanistic study carried out by our group has demonstrated that these interactions occur even at the beginning of the treatment. The detailed findings will be reported in another manuscript.
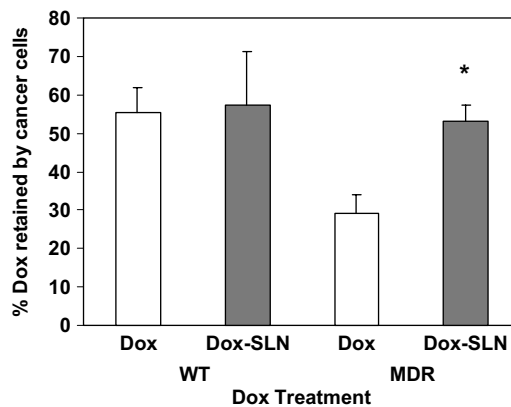

Fig. 11. Cellular retention of Dox by wild-type MDA435/LCC6/WT (WT) and P-gp-overexpressing MDA435/LCC6/MDR1 (MDR) breast cancer cell lines. Cells were treated with doxorubicin solution (Dox) or Dox-loaded solid lipid nanoparticles (Dox–SLN) for 2 h, rinsed with PBS three times to remove the treatments, and reincubated with fresh EBSS medium for 2 h ($t = 2$ h) to allow efflux of drug from the cells. Results are normalized against the values just prior to drug efflux ($t = 0$) and expressed as % Dox retained. Means of measurements of three independent experiments are presented. Error bar = SD. *$p < 0.05$ when compared to Dox treatment.

The biological activity of the drug was not altered after the loading and the release processes (Fig. 9), which is essential for a suitable drug delivery system. The components of the nanoparticle system, i.e., HPESO and Pluronic F68, exhibited very low membrane toxicity in the trypan blue exclusion assay experiments within 4 h (Figs. 7A and 6B). Therefore, any differences in the activity against cancer cell proliferation that were observed in the clonogenic experiments were likely attributable to the differences in the dosage forms rather than the cytotoxicity of the individual materials used in the Dox–SLN.

Pluronic (also known as poloxamer) copolymers were reported to have MDR reversal activity (41). However, the results of the combined treatment of blank SLN and Dox solutions suggested that the copolymer Pluronic F68 by itself did not play a significant role in the cytotoxicity. This observation may be explained by the high dilution of the SLN suspensions used in the *in vitro* experiments where the surfactant concentrations were quite low (0.0005–0.005% w/v). Besides, Pluronic F68 is relatively hydrophilic and has lower P-gp inhibitory activity among the Pluronic series (42). Therefore, by using this surfactant, the role of the nanoparticle itself can be more easily defined. We anticipate that if Pluronic F68 is replaced with another copolymer with stronger P-gp inhibitory effects (e.g., Pluronic P85) in the preparation of Dox–SLN, the cytotoxicity of the formulation against MDR cells may become more prominent.

The Dox–SLN formulation was significantly more cytotoxic to the MDR subline than the Dox solution, whereas it exhibited similar cancer-suppressive activity on the wild-type cell line as compared to the conventional Dox solution treatment (Fig. 10A and B). This additional activity was stronger than that conferred by Dox and the free polymer alone (Dox–polymer aggregates). The drug-loaded and the blank SLN did not change the cell membrane permeability within 4 h in the trypan blue exclusion assays (Fig. 8A and B), neither did the addition of blank SLN to Dox solutions (Fig. 10B). Hence, the possibilities that the lipid components may alter membrane permeability or are intrinsically chemo-sensitizing (24–26) are eliminated. These findings are different from those in a previous study with liposomes, where empty liposomes were able to render the free drug more effective on MDR cells (26).

When the Dox–HPESO complex was not formulated in the form of lipid nanoparticles and given by itself, it did not result in enhanced cytotoxicity to MDR cells, although it was more toxic than the free Dox to the wild-type cells (Fig. 10A and B). A possible explanation for the enhanced toxicity of the Dox–polymer aggregates to wild-type but not MDR cells may be due to the presence of some residual drug–polymer aggregates. Such drug–polymer aggregates could be seen under the microscope to be firmly adhered to the cells even after the cells were washed with PBS three times. It seemed that a fraction of the drug–polymer complex still remained attached onto the cells that were seeded in the Petri dishes for the clonogenic assay and served as mini depots for extended, low-level drug supply. For cells that are not drug resistant, this may result in significant toxicity, but for MDR cells, the drug concentration supplied by this additional source was not toxic.

The present study demonstrates that by combining the various components including the lipid, polymer, and Dox together into a single nanoparticle, i.e., Dox–SLN, the drug is more effective against drug-resistant cancer cells than when these components are used in a physically separated manner. This observation is consistent with the findings by Kreuter *et al.* (43), which showed that a drug had to be physically associated with polymeric nanoparticles to be efficiently delivered across the simulated P-gp-rich blood–brain barrier. To the best of our knowledge, this is the first report that clearly demonstrates the potential therapeutic advantage of an SLN system loaded with a water-soluble cytotoxic drug (e.g., Dox) in overcoming P-gp-mediated drug resistance in cancer cells. It may possibly open up more opportunities in terms of SLN applications in future.

There are two possibilities about the mechanism of cytotoxicity for Dox–SLN: 1) Dox is released from Dox–SLN outside the cells and works like free Dox, but its cytotoxicity is enhanced by the nanoparticles. 2) Dox is carried by the nanoparticles and released inside the cells, resulting in higher cytotoxicity. Cellular drug uptake study was conducted to shed light on this issue. The results of this study are, in general, consistent with the clonogenic assay data. Dox–SLN led to higher drug uptake in P-gp-overexpressing cells, but not in wild-type cells. The drug uptake of free Dox was not increased by the presence of blank SLNs. In other words, the possibility that the lipids or surfactants of SLNs enhance the effect of free Dox by exhibiting P-gp inhibitory effect can be ruled out. A part of the Dox delivered by Dox–SLNs was likely taken up by the cells using alternate mechanisms that bypass P-gp drug efflux. In fact, it was shown in the drug retention study (Fig. 11) that the Dox in SLN taken up by the cells is more difficult to be cleared by the P-gp efflux mechanism. In our initial studies using fluorescence microcopy, the drugs and lipids were found actually both internalized and did not just adhere on the cell surface (data not shown here). Endocytosis of nanoparticles by the tumor cells may occur, as suggested previously in some studies using polymeric nanoparticle systems (26,27,44). The endocytosed form of Dox–SLN is likely more difficult to be removed by the membrane-associated mechanism such as P-gp drug efflux. A more detailed mechanistic study was conducted in our laboratory to further delineate these issues from which a manuscript has been resulted (Wong *et al.*, unpublished data).

CONCLUSION

A new polymer–lipid hybrid nanoparticle system containing polymer–Dox complex was prepared and evaluated for its *in vitro* cytotoxicity toward wild-type and MDR human breast tumor cell lines. The Dox–SLN showed much higher *in vitro* cytotoxicity against the P-gp overexpressing cell line but no difference on a wild-type cell line when compared to free Dox solutions. This enhanced cytotoxicity was not attributable to the loss of the cell membrane integrity and was not caused by the individual components in the formulation. Instead the integration of the drug, the polymer, and the lipid in a nanoparticle form is essential for the enhanced cytotoxicity, drug uptake, and retention. These data suggest that the new polymer–lipid hybrid nanoparticle system may offer great potential to deliver Dox effectively for the treatment of MDR breast cancer.

REFERENCES

1. P. E. Lonning. Study of suboptimum treatment response: lessons from breast cancer. *Lancet Oncol.* **4**:177–185 (2003).
2. Early Breast Cancer Trialists' Collaborative Group. Polychemotherapy for early breast cancer: an overview of the randomized trials. *Lancet* **352**:930–942 (1998).
3. M. M. Gottesman. Mechanisms of cancer drug resistance. *Annu. Rev. Med.* **53**:615–627 (2002).
4. F. Leonessa and R. Clarke. ATP binding cassette transporters and drug resistance in breast cancer. *Endocr.-Relat. Cancer* **10**:43–73 (2003).
5. I. Mohamed and R. T. Skeel. Carcinoma of breast. In R. T. Skeel (ed.), *Handbook of Cancer Chemotherapy*, Lippincott Williams & Wilkins, Philadelphia, 2003, pp. 269–293.
6. H. C. Chung, S. Y. Rha, J. H. Kim, J. K. Roh, J. S. Min, K. S. Lee, B. S. Kim, and K. B. Lee. P-glycoprotein: the intermediate end point of drug response to induction chemotherapy in locally advanced breast cancer. *Breast Cancer Res. Tr.* **42**:65–72 (1967).
7. Z. Liu, X. Y. Wu, and R. Bendayan. *In vitro* investigation of ionic polysaccharide microspheres for simultaneous delivery of chemosensitizer and antineoplastic agent to multidrug-resistant cells. *J. Pharm. Sci.* **88**:412–418 (1999).
8. R. Y. Cheung, A. M. Rauth, and X. Y. Wu. *In vivo* efficacy and toxicity of intratumorally delivered mitomycin C and its combination with doxorubicin using microsphere formulations. *Anti-Cancer Drugs* **16**(4):423–433 (2005).
9. R. Cheung, Y. Ying, A. M. Rauth, N. Marcon, and X. Y. Wu. Biodegradable dextran-based microspheres for delivery of anticancer drug mitomycin C. *Biomaterials* **26**:5375–5385 (2005).
10. Z. Liu, R. Cheung, X. Y. Wu, J. R. Ballinger, R. Bendayan, and A. M. Rauth. A study of doxorubicin loading onto and release from sulfopropyl dextran ion-exchange microspheres. *J. Control. Release* **77**:213–224 (2001).
11. S. C. J. Steiniger, J. Kreuter, A. S. Khalansky, I. N. Skidan, A. I. Bobruskin, Z. S. Smirnova, S. E. Severin, R. Uhl, M. Kock, K. D. Geiger, and S. E. Gelperina. Chemotherapy of glioblastoma in rats using doxorubicin-loaded nanoparticles. *Int. J. Cancer* **109**:759–767 (2004).
12. S. E. Gelperina, A. S. Khalansky, I. N. Skidan, Z. S. Smirnova, A. I. Bobruskin, S. E. Severin, B. Turowski, F. E. Zanella, and J. Kreuter. Toxicological studies of doxorubicin bound to polysorbate 80-coated poly(butyl cyanoacrylate) nanoparticles in healthy rats and rats with intracranial glioblastoma. *Toxicol. Lett.* **126**:131–141 (2002).
13. M. I. Koukourakis, S. Koukouraki, I. Fezoulidis, G. Kurias, S. Archimandritis, and N. Karkavitsas. High intratumoral accumulation of stealth liposomal doxorubicin (Caelyx) in glioblastomas and in metastatic tumours. *Br. J. Cancer* **83**:1281–1286 (2000).
14. U. Massing and S. Fuxius. Liposomal formulations of anticancer drugs: selectivity and effectiveness. *Drug Resist. Updat.* **3**:171–177 (2000).
15. Z. Liu, J. R. Ballinger, A. M. Rauth, R. Bendayan, and X. Y. Wu. Delivery of an anticancer drug and a chemosensitizer to murine breast sarcoma by intratumoral injection of sulfopropyl

16. dextran microspheres. *J. Pharm. Pharmacol.* **55**:1063–1073 (2003).
17. Z. Liu, R. Bendayan, and X. Y. Wu. Triton-X-100-modified polymer and microspheres for reversal of multidrug resistance. *J. Pharm. Pharmacol.* **53**:1–12 (2001).
18. Z. Liu, X. Y. Wu, and R. Bendayan. *In vitro* investigation of ionic polysaccharide microspheres for simultaneous delivery of chemosensitizer and antineoplastic agent to multidrug-resistant cells. *J. Pharm. Sci.* **88**:412–418 (1999).
19. J. Huwyler, A. Cerletti, G. Fricker, A. N. Eberle, and J. Drewe. By-passing of P-glycoprotein using immunoliposomes. *J. Drug Target.* **10**:73–79 (2002).
20. C. Mamot, D. C. Drummond, K. Hong, D. B. Kirpotin, and J. W. Park. Liposome-based approaches to overcome anticancer drug resistance. *Drug Resist. Updat.* **6**:271–279 (2003).
21. C. E. Soma, C. Dubernet, D. Bentolila, S. Benita, and P. Couvreur. Reversion of multidrug resistance by co-encapsulation of doxorubicin and cyclosporin A in polyalkylcyanoacrylate nanoparticles. *Biomaterials* **21**:1–7 (2000).
22. L. Fenart, A. Casanova, B. Dehouck, C. Duhem, S. Slupek, R. Cecchelli, and D. Betbeder. Evaluation of effect of charge and lipid coating on ability of 60 nm nanoparticles to cross an *in vitro* model of the blood–brain barrier. *J. Pharmacol. Exp. Ther.* **291**:1017–1022 (1999).
23. A. C. Verdierede, C. Dubernet, F. Nemati, E. Soma, M. Appel, J. Ferte, S. Bernard, F. Puisieux, and P. Couvreur. Reversion of multidrug resistance with polyalkylcyanoacrylate nanoparticles: towards a mechanism of action. *Br. J. Cancer* **76**:198–205 (1997).
24. C. E. Soma, C. Dubernet, G. Barratt, F. Nemati, M. Appel, S. Benita, and P. Couvreur. Ability of doxorubicin-loaded nanoparticles to overcome multidrug resistance of tumor cells after their capture by macrophages. *Pharm. Res.* **16**:1710–1716 (1999).
25. A. R. Thierry, D. Vige, S. S. Coughlin, J. A. Belli, A. Dritschilo, and A. Rahman. Modulation of doxorubicin resistance in multidrug-resistant cells by liposomes. *FASEB J.* **7**:572–579 (1993).
26. Y. Romsicki and F. J. Sharom. The membrane lipid environment modulates drug interactions with the P-glycoprotein multidrug transporter. *Biochemistry* **38**:6887–6896 (1999).
27. Y. L. Lo. Phospholipids as multidrug resistance modulators of the transport of epirubicin in human intestinal epithelial Caco-2 cell layers and everted gut sacs of rats. *Biochem. Pharmacol.* **60**:1381–1390 (2000).
28. R. H. Muller, K. Mader, and S. Gohla. Solid lipid nanoparticles (SLN) for controlled drug delivery—a review of the state of the art. *Eur. J. Pharm. Biopharm.* **50**:161–177 (2000).
29. R. H. Muller, D. Ruhl, S. Runge, K. Schulze-Forster, and W. Mehnert. Cytotoxicity of solid lipid nanoparticles as a function of the lipid matrix and the surfactant. *Pharm. Res.* **14**:458–462 (1997).
30. J. M. Koziara, P. R. Lockman, D. D. Allen, and R. J. Mumper. Paclitaxel nanoparticles for the potential treatment of brain tumors. *J. Control. Release* **99**:259–269 (2004).
31. R. Cavalli, O. Caputo, and M. R. Gasco. Solid lipospheres of doxorubicin and idarubicin. *Int. J. Pharm.* **89**:R9–R12 (1993).
32. L. Serpe, M. G. Catalano, R. Cavalli, E. Ugazio, O. Bosco, R. Canaparo, E. Muntoni, R. Frairia, M. R. Gasco, M. Eandi, and G. P. Zara. Cytotoxicity of anticancer drugs incorporated in solid lipid nanoparticles on HT-29 colorectal cancer cell line. *Eur. J. Pharm. Biopharm.* **58**:673–680 (2004).
33. A. Miglietta, R. Cavalli, C. Bocca, L. Gabriel, and M. R. Gasco. Cellular uptake and cytotoxicity of solid lipid nanospheres (SLN) incorporating doxorubicin or paclitaxel. *Int. J. Pharm.* **210**:61–67 (2000).
34. S. M. Hahn, A. Russo, J. A. Cook, and J. B. Mitchell. A multidrug-resistant breast cancer line induced by weekly exposure to doxorubicin. *Int. J. Oncol.* **14**:273–279 (1999).
35. H. L. Wong, R. Bendayan, A. M. Rauth, and X. Y. Wu. Development of solid lipid nanoparticles containing ionically-complexed chemotherapeutic drugs and chemosensitizers. *J. Pharm. Sci.* **93**:1993–2004 (2004).
36. F. Leonessa, D. Green, T. Licht, A. Wright, K. Wingate-Legette, J. Lippman, M. M. Gottesman, and R. Clarke. MDA435/LCC6 and MDA435/LCC6^{MDR1}: ascites models of human breast cancer. *Br. J. Cancer* **73**:154–161 (1996).

36. R.G. Bristow and R.P. Hill. Molecular and cellular basis of radiotherapy. In I. F. Tannock and R. P. Hill (eds.), *The Basic Science of Oncology*, McGraw-Hill, Toronto, 1998, pp. 295–321.

37. Z. Liu and S. Erhan. Synthesis and properties of new soybean oil based polymers, US patent application.

38. D. Z. Hou, C. S. Xie, K. J. Huang, and C. H. Zhu. The production and characteristics of solid lipid nanoparticles (SLNs). *Biomaterials* **24**:1781–1785 (2003).

39. J. Moselhy, X. Y. Wu, R. Nicholov, and K. Kodaria. *In vitro* characterization of interaction of poly(NIPAm/MAA) nanoparticles with proteins and cells. *J. Biomater. Sci. Polym. Ed.* **11**:123–147 (2000).

40. S. L. Abrahamse, B. L. Pool-Zobel, and G. Rechkemmer. Potential of short chain fatty acids to modulate the induction of DNA damage and changes in the intracellular calcium concentration by oxidative stress in isolated rat distal colon cells. *Carcinogenesis* **20**:629–634 (1999).

41. A. V. Kabanov, E. V. Batrakova, and V. Y. Alakhov. Pluronic block copolymers for overcoming drug resistance in cancer. *Adv. Drug Deliv. Rev.* **54**:759–779 (2002).

42. E. V. Batrakova, S. Lee, S. Li, A. Venn, V. Alakhov, and A. Kabanov. Fundamental relationships between the composition of pluronic block copolymers and their hypersensitization effect in MDR cancer cells. *Pharm. Res.* **16**:1373–1379 (1999).

43. J. Kreuter, P. Ramge, V. Petrov, S. Hamm, S. E. Gelperina, B. Engelhardt, R. Alyautdin, H. von Briesen, and D. J. Begley. Direct evidence that polysorbate-80-coated poly(butylcyanoacrylate) nanoparticles deliver drugs to the CNS via specific mechanisms requiring prior binding of drug to the nanoparticles. *Pharm. Res.* **20**:409–416 (2003).

44. A. Tang, P. Kopeckova, and J. Kopecek. Binding and cytotoxicity of HPMA copolymer conjugates to lymphocytes mediated by receptor-binding epitopes. *Pharm. Res.* **20**:360–367 (2003).